CO_2 and H_2 Gas Mixture Inclusion Effect on Shrinkage of Ar Induction Thermal Plasmas

Sharif Abdullah Al-Mamun Student Member (Kanazawa University)
Yasunori Tanaka Member (Kanazawa University)
Yoshihiko Uesugi Member (Kanazawa University)

Keywords: inductively coupled thermal plasma, molecular gas mixture, plasma radius, shrinkage

1. Introduction

In thermal plasma technology, some molecular gas mixtures are used for working gases. On the other hand it is well known that SF_6 has high global warming potential. So in the circuit breaker fields, alternatives for SF_6 are being searched as an arc quenching gas from the viewpoint of an environmental issue. The CO_2 or additional gas added CO_2 is one of the candidates for such arc quenching gases. In order to investigate its fundamental properties, the inductively coupled thermal plasma technique is useful because of free from any contamination. In the present work, effect of CO_2+H_2 gas mixture inclusion was numerically investigated on high power Ar inductively coupled thermal plasmas at atmospheric pressure.

2. Calculation Condition

Simulation has been carried out solving a two-dimensional local thermodynamic equilibrium (LTE) code. Calculation was performed for the high power radio frequency ICTP system setup installed in the laboratory shown in Fig. 1. The active plasma power and input fundamental frequency were 27 kW and 450 kHz respectively. The numerical calculation was carried out using SIMPLE algorithm with uniform grid system having 66 radial and 92 axial nodes. The thermodynamic and transport properties had been derived from thermal plasma composition calculated by Gibb's energy minimization (GEM). Using the equilibrium composition, the thermodynamic properties such as mass density, enthalpy, and specific heat at constant pressure were calculated from partition function. Also, with the equilibrium composition and collision cross section data, the transport properties including viscosity, electrical and thermal conductivity were calculated by the first order approximation of Chapman-Enskog method. Figure 2 shows the Variation of specific heat and thermal conductivity for different gases as a function of temperature. Calculation conditions are listed in Table 1. The main variable parameter was the admixture ratio of secondary gas (CO_2+H_2 gas mixture).

3. Results

It has been found that the injection of excess dissociative molecular gases shrink the plasma (salender plasma column) in radius keeping the center temperature about 9–10 kK as shown in Fig. 3. The result shows that inclusion of secondary molecular gas mixture of CO_2+H_2 causes the shrink of plasma torch and increasing the admixture ratio of molecular gas further shrinks it. It can be found easily if we define 'plasma radius' having temperature beyond 5000 K for each of the cases. The result is also compared with that of Ar-CO_2 and Ar-H_2 tharmal plasma and finally a comparative study and conclusion had been made.

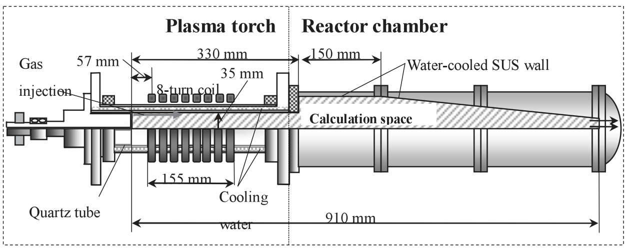

Fig. 1. Plasma torch configuration

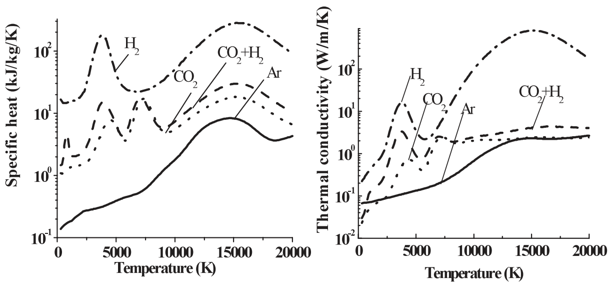

Fig. 2. Variation of specific heat and thermal conductivity for different gases as a function of temperature

Table 1. Calculation conditions

Input power = 30 kW
Active plasma power = 27 kW
Pressure = 0.1 MPa (atmospheric)
Frequency = 450 kHz
Volume ratio of CO_2 : H_2 gas mixture: 1: 1 (50% each)
Flow rate: Case 1. Ar = 100 slpm (standard liter per minute); Case 2. Ar = 98 slpm, CO_2+H_2 = 2 slpm; Case 3. Ar = 96 slpm, CO_2+H_2 = 4 slpm; Case 4. Ar = 94 slpm, CO_2+H_2 = 6 slpm; Case 5. Ar = 92 slpm, CO_2+H_2 = 8 slpm; Case 6. Ar = 90 slpm, CO_2+H_2 = 10 slpm

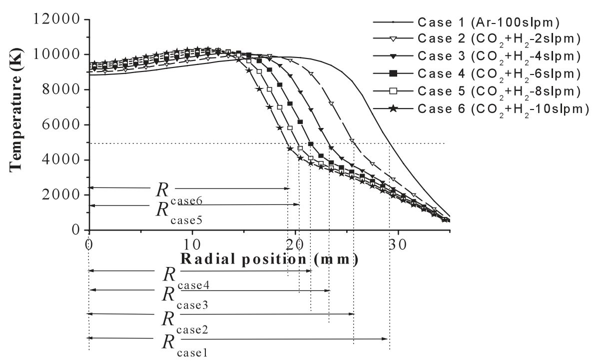

Fig. 3. Radial temperature distribution for all cases at axial position of z = 155 mm

Paper

CO_2 and H_2 Gas Mixture Inclusion Effect on Shrinkage of Ar Induction Thermal Plasmas

Sharif Abdullah Al-Mamun[*] Student Member
Yasunori Tanaka[*] Member
Yoshihiko Uesugi[*] Member

In the present work, effect of CO_2+H_2 gas mixture inclusion on shrinkage of plasma was numerically investigated on high power Ar inductively coupled thermal plasmas at atmospheric pressure. The gas mixture of CO_2+H_2 has many reactions in wide temperature range of 300–20000 K which may cause some performance in thermal plasmas. Simulation has been carried out solving a two-dimensional local thermodynamic equilibrium (LTE) code. The active plasma power and input fundamental frequency were fixed at 27 kW and 450 kHz respectively. The main variable parameter was the admixture ratio of secondary gas (CO_2+H_2 gas mixture) and it has been found that the injection of excess dissociative molecular gases shrink the plasma in radius keeping the center temperature about 10,000 K by investigating the plasma radius having temperature beyond 5,000 K for each of the case. The result also shows that increasing the inclusion (admixture ratio) of CO_2+H_2 molecular gas raises the plasma peak temperature. The result is also compared with that of Ar-CO_2 and Ar-H_2 thermal plasma and finally a comparative study and conclusions have been made.

Keywords: inductively coupled thermal plasma, molecular gas mixture, plasma radius, shrinkage

1. Introduction

Nowadays, a great attention has been paid to mixed gas inductively coupled thermal plasmas (ICTP) for their bright prospect especially in surface modification, material processing and investigation of steady and transient quenching property of molecular gases. It has distinctive feature of high energy density, chemical reactivity and variable transport properties. For example, Ar+N_2+CO_2 are tried to adapt to thermal plasma treatment for improving anode electrode performance in Li battery [1].

On the other hand, it is well known that SF_6 is used as an arc quenching medium in the high voltage circuit breaker. SF_6 gas has the attractive arc quenching property ever found among almost all gases. There seems to have mainly two reasons behind it. Firstly, high thermal conductivity of SF_6 at low temperature (around 2000 K) makes the thermal plasma column slender shape which leads the plasma to have fast dynamic response in changing its conductance. Secondly, SF_6 and its products have high electron attachment cross sections that cause a decrease in electron density and thus the plasma temperature [2]. However, SF_6 has high global warming potential. So in the circuit breaker fields, alternatives for SF_6 are being searched as an arc quenching gas from the viewpoint of an environmental issue. The CO_2 or additional gas added CO_2 is one of the candidates for such arc quenching gases. CO_2 has a low global warming potential (GWP) as compared with SF_6 (1/23900 times). Moreover H_2 is environmentally benign and easily available in nature. Concerning about the air pollution and global warming, H_2 is considered as one of the arc quenching medium because of its high thermal conductivity. Thus CO_2+H_2 gas inclusion effect was investigated in this paper for fundamental study. In addition, CO_2+H_2 gas mixture is also related with polymer ablation vapor such as POM and PMMA used for dielectric insulation because these materials contain only C, H and O atoms.The polymer ablation is one of the key technique for low-voltage circuit breakers. We have studied plasma quenching efficiency of gas using inductively coupled thermal plasma (ICTP) technique. The ICTP technique has some advantages for fundamental and comparative study of gas-plasma interactions both in numerical and experimental approaches [2] since it is free from any contamination. Thus CO_2+H_2 gas inclusion effect was investigated in this paper. We have studied plasma quenching efficiency of gas using ICTP technique. On the other hand, other researchers have been studying both the steady state and transient response for argon mixed with single molecular gas ICTP. For example, Nishiyama et al. [3], Cai et al. [4] and Bourg et al. [5] investigated the temperature and flow field for Ar-He, Ar-O_2, Ar-N_2 and Ar-H_2 thermal plasmas in steady state. And then dynamic characteristics and also non-equilibrium analysis have been made for argon with single molecular gas [6]. Ar-CO_2 and Ar-H_2 radio frequency ICTP simulation has been executed already. However, Ar-CO_2-H_2 thermal plasma ICTP has not been done yet because of complexity of its transport and thermodynamic properties.

The shrinkage of thermal plasma is a very significant parameter to be considered now-a-days, especially in high power gas circuit breakers. Because, it has been found that slendered plasma column leads to have fast dynamic behaviour in changing its conductance that causes high plasma

[*] Div. of Electrical Eng. & Computer Sci., Kanazawa University
Kakuma-machi, Kanazawa 920-1192

quenching efficiency [2]. Generally, shrinkage of plasma means the eshtablishment of narrower or thin thermal plasma with low radius.

In the present work, we did numerical simulation to predict differences in temperature fields and plasma shrinkage as a function of admixture ratio of secondary gas for Ar-CO_2-H_2 induction thermal plasma under local thermal equilibrium condition. Thus, we show the effect of molecular gas inclusion on plasma shrinkage phenomena, and then the controllability of plasma temperature and gas flow field by changing admixing ratio of molecular gas mixture (secondary gases) in ICTP.

2. Simulation Details

2.1 Assumption and Governing Equations In the present work, the plasma is under LTE condition, assumed to be optically thin so that light absorption can be neglected. Two-dimensional, laminar, steady and axisymmetric plasma flow has been considered and also viscous dissipation is negligible.

Electron temperature is assumed to be equal to that of heavy particles. Under the assumptions mentioned above, the present model is derived from conservation equations along with two-dimensional vector potential form of Maxwell's equation. The governing equations are as follows:

Mass conservation

$$\frac{\partial(\rho u)}{\partial z} + \frac{1}{r}\frac{\partial(\rho r v)}{\partial r} = 0 \quad \cdots\cdots (1)$$

Momentum conservation

Axial momentum

$$\frac{\partial(u\rho u)}{\partial z} + \frac{1}{r}\frac{\partial(rv\rho u)}{\partial r} = -\frac{\partial p}{\partial z} + 2\frac{\partial}{\partial z}\left(\eta\frac{\partial u}{\partial z}\right) + \frac{1}{r}\frac{\partial}{\partial r}\left[\eta r\left(\frac{\partial u}{\partial r} + \frac{\partial v}{\partial z}\right)\right] + F_z \quad \cdots\cdots (2)$$

Radial momentum

$$\frac{\partial(u\rho v)}{\partial z} + \frac{1}{r}\frac{\partial(rv\rho v)}{\partial r} = -\frac{\partial p}{\partial r} + \frac{\partial}{\partial z}\left[\eta\left(\frac{\partial v}{\partial z} + \frac{\partial u}{\partial r}\right)\right] + \frac{2}{r}\frac{\partial}{\partial r}\left[\eta r\left(\frac{\partial v}{\partial r}\right)\right] + F_r \quad \cdots\cdots (3)$$

Tangential (swirl) momentum

$$\frac{\partial(u\rho w)}{\partial z} + \frac{1}{r}\frac{\partial(rv\rho w)}{\partial r} = \frac{\partial}{\partial z}\left(\eta\frac{\partial w}{\partial z}\right) + \frac{1}{r}\frac{\partial}{\partial r}\left(\eta r\frac{\partial w}{\partial r}\right) - \frac{\rho v w}{r} - \frac{1}{r}\frac{\partial(\eta w)}{\partial r} + \eta\frac{\partial}{\partial r}\left(\frac{w}{r}\right) \quad \cdots\cdots (4)$$

Energy conservation

$$\frac{\partial(u\rho h)}{\partial z} + \frac{1}{r}\frac{\partial(rv\rho h)}{\partial r} = \frac{\partial}{\partial z}\left(\frac{k}{C_p}\frac{\partial h}{\partial z}\right) + \frac{1}{r}\frac{\partial}{\partial r}\left(\frac{k}{C_p}r\frac{\partial h}{\partial r}\right) + P^o - R^o \quad \cdots\cdots (5)$$

Vector potential form of Maxwell's equation

$$\dot{A}_\theta = A_R + jA_I \quad \cdots\cdots (6)$$

$$\frac{\partial^2 \dot{A}_\theta}{\partial z^2} + \frac{1}{r}\frac{\partial}{\partial r}\left(r\frac{\partial \dot{A}_\theta}{\partial r}\right) - \frac{\dot{A}_\theta}{r^2} = j\mu_0\sigma\omega\dot{A}_\theta \quad \cdots\cdots (7)$$

where, u, v and w: velocity in z-axis (axial), r-axis (radial) and tangential (swirl) components in m/s; σ: electrical conductivity in S/m; k: thermal conductivity in W/m/K, ρ: density in kg/m^3; C_p: specific heat in kJ/m^3/K; h: enthalpy in J/kg; p: pressure in Pa; η: viscosity in Pa·s; μ_0 : permeability of vacuum in H/m; Fz and F_r: Axial and radial components of Lorentz forces respectively in N/m^3; P^o: volumetric joule heating in W/m^3; R^o: volumetric radiation loss in W/m^3; A_θ: phasor of vector potential in A/m; ω: angular velocity in rad/s ($\omega = 2\pi f$, where f is the frequency of coil current); and j: complex operator.

2.2 Schematic and Calculational Domain Calculation was performed for the high power radio frequency ICTP system setup installed in the laboratory. The schematic configuration with calculation space of the high power ICP system is shown in Fig. 1. The setup comprises of two basic parts namely (a) plasma torch and (b) reaction chamber. The plasma torch portion is made up with two coaxial quartz tubes of 3.0 mm thickness. Between the gaps of the tubes, cooling water at room temperature flows for efficient cooling of tube wall. The inner diameter and length of plasma torch are 70 mm and 330 mm respectively. Along the inside tube wall, Ar-CO_2-H_2 gas mixture is supplied as a sheath gas. A winding of eight turn induction coil is installed around the

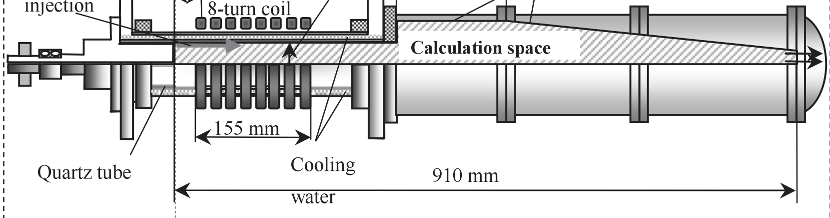

Fig. 1. Plasma torch configuration and calculation space

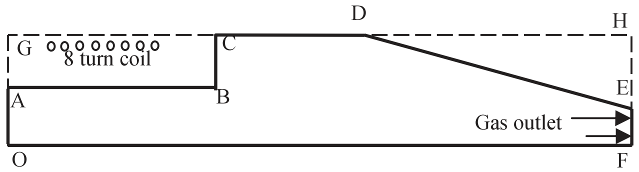

Fig. 2. Calculational domain

Table 1. Operating conditions

Input power = 30 kW
Active plasma power = 27 kW
Pressure = 0.1 MPa (atmospheric)
Frequency = 450 kHz
Volume ratio of CO_2 : H_2 gas mixture: 1: 1 (50% each) at 300 K
Flow rate(Admixture ratio): Case 1. Ar = 100 slpm (standard liter per minute)(100%Ar); Case 2. Ar = 98 slpm, CO_2+H_2 = 2 slpm(98%Ar-1%CO_2-%H_2); Case 3. Ar = 96 slpm, CO_2+H_2 = 4 slpm(96%Ar-2%CO_2-2%H_2); Case 4. Ar = 94 slpm, CO_2+H_2 = 6 slpm(94%Ar-3%CO_2-3%H_2); Case 5. Ar = 92 slpm, CO_2+H_2 = 8 slpm(92%Ar-4%CO_2-4%H_2); Case 6. Ar = 90 slpm, CO_2+H_2 = 10 slpm(90%Ar-5%CO_2-5%H_2) (gas injection temperature is 300 K)

plasma torch. A high frequency coil current (450 kHz) with an input power of 30 kW is fed to the system to produce and sustain steady plasma inside the plasma torch.

Figure 2 shows the calculational domain where O-A-B-C-D-E-F is the calculational space inside which fluid parameters and scalar quantities were evaluated. The two-dimensional space co-ordinate are O(0, 0), A(0, 35), B(330, 35), C(330, 65), D(480, 65), E(910, 20) and F(910, 0) where the unit is in mm. The operating conditions are listed in Table 1.

The numerical calculation was carried out using SIMPLE algorithm with uniform grid system having 66 radial and 92 axial nodes.

2.3 Calculation of Composition and Gas Properties

2.3.1 Equilibrium composition of Ar-CO_2-H_2

Equilibrium composition of Ar-CO_2-H_2 thermal plasma was calculated by minimization of Gibb's free energy of a system including Ar, CO_2 and H_2. Thermo-chemical properties were taken from JANAF thermo chemical tables [7]. Figure 3 shows the equilibrium composition of 98%Ar-1%CO_2-1%H_2 plasma at a pressure of 0.1 MPa as an example. Around 300 K, CO_2, H_2O, CH_4, H_2 are dominant species. This means that once gas mixture of CO_2+H_2 is decomposed, it do not recover CO_2 and H_2, but become another mixture of CO_2, H_2O, CH_4 and H_2 due to minimization of energy of the system. On the other hand, increasing temperature from 300 to 1000 K, CH_4 is dissociated rapidly, and then H atoms are produced. From 1000 to 3000 K, densities of H, OH, O and O_2 increase. In 3000–9000 K, molecules are dissociated and, H is dominant species. These many species and reactions causes complex thermodynamic and transport properties of CO_2+H_2 mixture.

2.3.2 Calculation of thermodynamic and transport properties The thermodynamic and transport properties that are prerequisite for any modeling had been derived using thermal plasma composition as a function of temperature. Using the equilibrium composition, the thermodynamic properties such as mass density, enthalpy, and specific heat at constant pressure were calculated with partition function as a function of temperature. Also, with the equilibrium composition and collision cross section data, the transport properties including viscosity, electrical and thermal conductivity were calculated as a function of temperature by the first order approximation of Chapman-Enskog method [8]. Figures 4 and 5 show the variation of specific heat and thermal conductivity of Ar, CO_2, CO_2-H_2 mixture of different ratios and H_2 respectively as a function of temperature. Figure 4 shows that there are inherent peaks in specific heat around 4000 K, 7000 K and 15000 K for CO_2 and CO_2+H_2 gas mixture with one extra peak around 1000 K for CO_2-H_2 only. This is due to the dissociation/formation of H_2O and CH_4. For H_2, the peaks are around 4000 K and 15000 K. At these temperatures, dissociation and ionization reactions are taken place and majority of energy is spent to dissociate and ionize the particles. H_2 has a very large specific heat per unit mass at the mentioned temperatures as compared to others. Thermal conductivity as shown in Fig. 5 also shows the similar nature to specific heat in terms of periodic peaks.

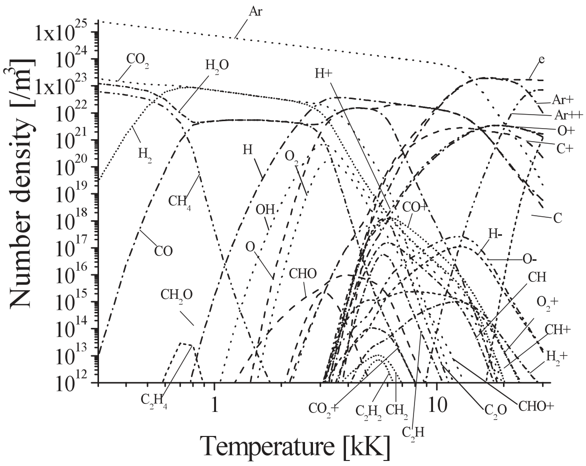

Fig. 3. Equilibrium composition of 98%Ar-1%CO_2-1%H_2 plasmas at atmospheric pressure

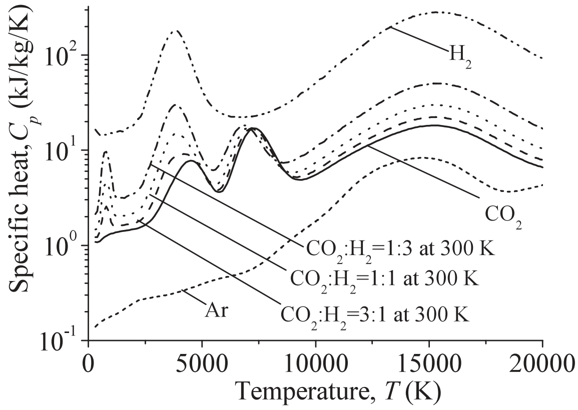

Fig. 4. Specific heat per unit mass for different gases of Ar, CO_2, H_2, and CO_2-H_2 mixture as a function of temperature at atmospheric pressure

2.4 Boundary Conditions As referred to Fig. 2, for

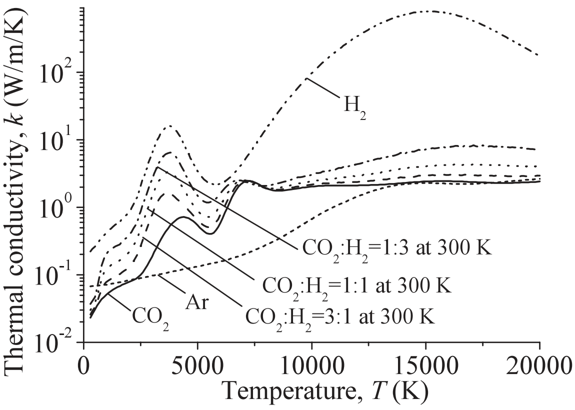

Fig. 5. Thermal conductivity for different gases of Ar, CO_2, H_2, and CO_2-H_2 mixture as a function of temperature at atmospheric pressure

the details of necessary boundary conditions readers are referred to Ref. (6).

For O-F line, we set derivatives of physical parameters such as axial gas velocity, swirl gas velocity and enthalpy while radial gas velocity and vector potential would be zero. For walls OA, AB, and B-C-D-E, we set gas velocities as zero and the temperature is calculated considering heat transfer from the wall. Vector potentials are calculated at GA, GC, DH and HF and around the coil. We set vector potential to be zero for metallic walls OA, B-C-D-E.

3. Calculational Results and Discussions

3.1 Gas Flow Field Figure 6 shows the obtained streamlines that indicate the profile of gas flow fields. The gas flows tangentially to the streamlines.

The streamlines are drawn at an interval of 10^{-3} kgm^{-2}s^{-1} for the stream function. Here, only three figures out of six cases are outlined as examples. The gas is injected as sheath gas along the internal wall of the quartz tube. Along z = 100 mm, the gas flow is bent to the radial direction due to the Lorentz force produced as an interaction between magnetic field of the coil current and eddy current inside the thermal plasma. Increasing admixture ratios of CO_2 and H_2 gas mixture to Ar cause more bending of gas flow to the radial direction.

3.2 Temperature Field Figure 7 demonstrates the iso-contour of temperature field for only the three cases already shown in streamline figures. Investigation of the plasma torch region shows that plasma shrinks as the admixture ratio of CO_2-H_2 increases. This phenomenon can be observed more clearly in Fig. 8 showing the radial distribution of temperature at axial position of z = 155 mm. If we can define "thermal plasma radius" as the radius of high temperature region above 5000 K at the axial position of 155 mm, we can see the plasma shrinkage effect of CO_2-H_2 gas mixture inclusion on Ar ICTP. Figure 9 shows the thermal plasma radius, R, of 5000 K as a function of CO_2-H_2 admixture ratio to Ar. Then we see that increasing CO_2-H_2 admixture ratio decreases the thermal plasma radius R. The thermal plasma radius decreases with CO_2+H_2 admixture ratio with decaying rate of 1 mm/%. This can be shown from figure 8 that the decaying rate is 0.99 ($\approx$ 1) mm/% [(29.1 − 19.2) mm/(10 − 0)%].

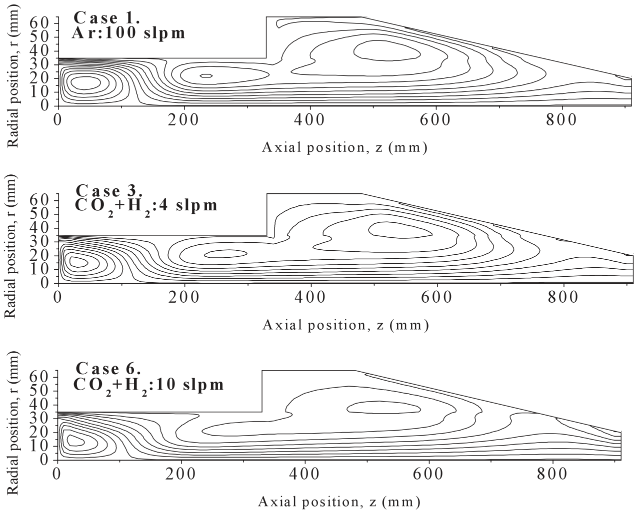

Fig. 6. Streamlines for gas flow field in 100%Ar, 96%Ar-2%CO_2-2%H_2 and 90%Ar-5%CO_2-5%H_2 plasmas

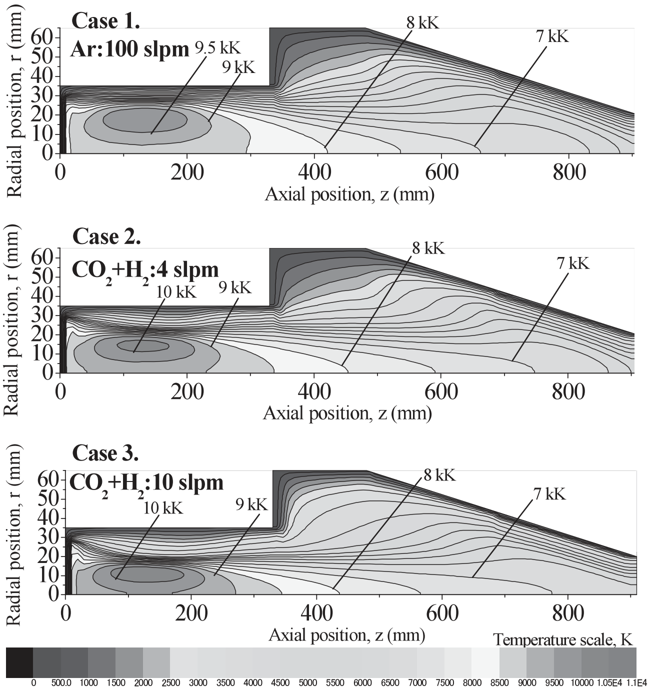

Fig. 7. Temperature field in 100%Ar, 96%Ar-2%CO_2-2%H_2 and 90%Ar-5%CO_2-5%H_2 plasmas

From Figs. 7 and 8, we found increased maximum temperature of Ar thermal plasma. Figure 10 shows the maximum temperature for all cases. The peak temperature inside the thermal plasma is the highest for the maximum admixing ratio of secondary gas (10 slpm).

3.3 Electrical Field Strength, Electrical Conductivity and Joule Heating Power Figure 11 shows the iso-contours of absolute value of electrical field strength for the three cases. This figure demonstrates that electric field strength is high near the wall and maximum at the coils but nearly zero at the axis of plasma torch. It is also observed that electric field increases and penetrates more inside the plasma core as admixture ratio of CO_2-H_2 increases. High admixture

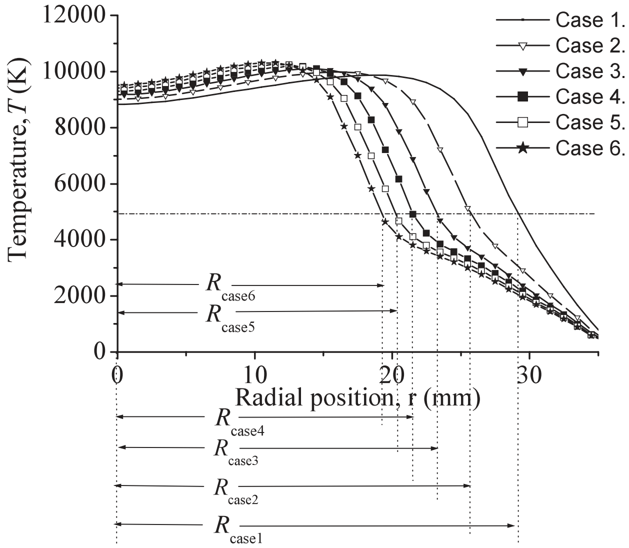

Fig. 8. Radial temperature distributions at axial position of z = 155 mm for 100%Ar, and Ar-CO_2-H_2 plasmas. Admixture ratio of secondary gas mixture CO_2-H_2 to Ar is taken as a parameter

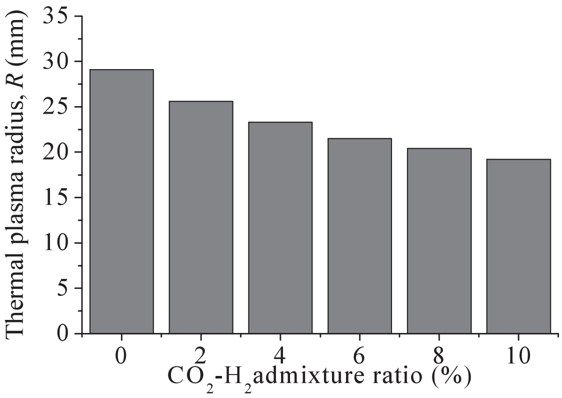

Fig. 9. Thermal plasma radii defined by 5000 K for different admixture ratio of CO_2-H_2

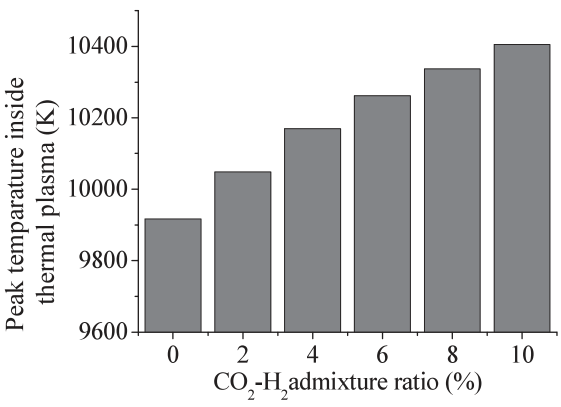

Fig. 10. Maximum temperature in plasma for 100%Ar, and Ar-CO_2-H_2 plasmas

ratio causes high electric field strength that accelerates electrons near the wall to enhance the electron kinetic energy. As a result eddy current increases which further intensifies the Lorentz force acting on the gas mixture that causes bending

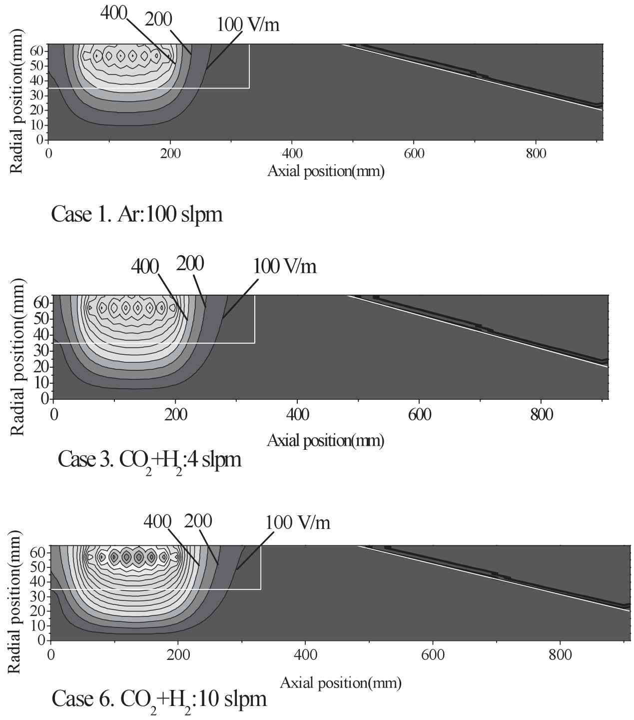

Fig. 11. Absolute value of electrical field strength (for three cases); white line shows the boundary of vacuum chamber

of gas flow to the radial direction.

Increasing admixture ratio of CO_2-H_2 causes the radial distribution of the electrical conductivity to be shrunk and become narrower to the core that is the main reason for concentrated joule heating for higher admixture ratio. CO_2-H_2 has higher specific heat per unit volume at low temperature that enhances the convection term of heat flow. This causes the shrinkage of plasma. So, the radius of electric conducting path inside plasma decreases. Also electrical conductivity increases and shrinks inside the core. As a result, current density increases that further causes increase of temperature. The eddy current also increases and the lorentz force due to the eddy current [6] also become larger that further drive the electrons and charged particles to the core of plasma.

3.4 Comparison Among Pure Ar, Ar-CO_2-H_2, Ar-CO_2 and Ar-H_2 Thermal Plasma Figure 12 demonstrates the radial temperature distribution for pure Ar, Ar-CO_2-H_2, Ar-CO_2 and Ar-H_2 thermal plasma. The admixture ratio for secondary gas in case of mixed gas plasmas was 10 slpm. In this figure also, we define the parameter of "thermal plasma radius" of the same definition stated before.

Thermal plasma radius is the highest for pure Ar plasma and decreases as we mix up molecular gas. Inclusion of CO_2 causes slight decrease of plasma radius, while inclusion of CO_2+H_2 gas mixture causes further shrink of plasma. But the mixing effect of H_2 is the most noticeable. Inclusion of H_2 causes a significant decrease of plasma radius implying a great shrink of plasma.

We can also explain these phenomena in terms of dacaying rate.

The value is maximum for Ar-H_2 (1.76 mm/%) and minimum for Ar-CO_2 (0.66 mm/%) as investigated from Fig. 12.

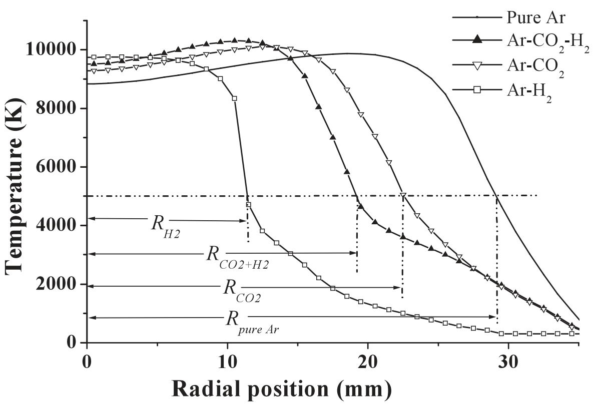

Fig. 12. Comparison of radial temperature distribution among pure Ar, Ar-CO_2-H_2, Ar-CO_2, and Ar-H_2 plasmas

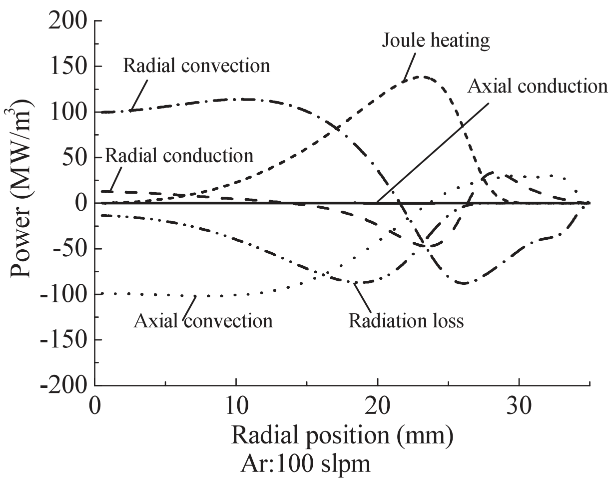

Fig. 13. Radial distribution of energy balance at an axial position of z = 155 mm for Ar-CO_2-H_2 thermal plasmas

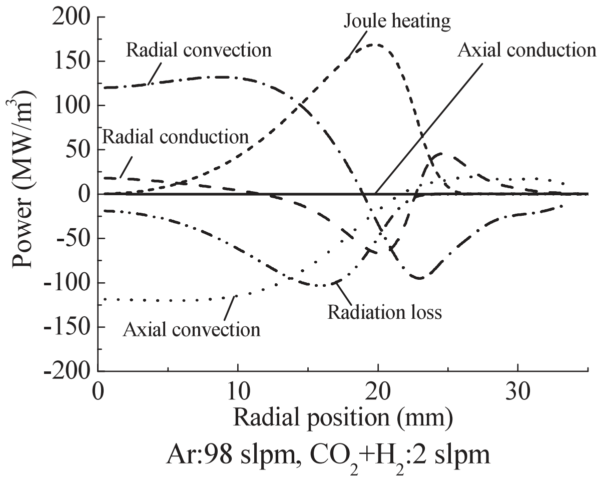

Fig. 14. Radial distribution of energy balance at an axial position of z = 155 mm for Ar-CO_2-H_2 thermal plasmas

3.5 Power Balance Figures 13 and 14 show radial distribution of various components of power flows and joule heating at an axial position of z = 155 mm for only pure Ar and Ar-CO_2-H_2 gas mixture. It is observed that an overall balance of power input and power loss is obtained that preserves the energy conservation law. For both cases, input power (in the form of electromagnetic power) by joule heating is transferred in radial direction by convection and conduction around r = 20 mm. Around the axis r = 0 mm, power is input from radial convection and then transferred by axial convection. In comparison with these two cases, Ar-CO_2-H_2 plasma has such a power transfer inner side than pure Ar plasma. Also, convection and conduction losses are higher in Ar-CO_2-H_2 plasma than pure Ar plasma.

4. Conclusions

It has been demonstrated that inclusion of secondary molecular gas causes the shrink of plasma torch. And increasing the admixture ratio of molecular gas further shrinks it. This is because it is evident that adding secondary molecular gases with pure Ar causes more chemical reactivity including ionization and dissociation reactions around the plasma temperature that greatly affects the thermodynamic and transport properties especially the specific heat and thermal conductivity of plasma gas.

(Manuscript received Aug. 1, 2006,
revised Aug. 13, 2007)

References

(1) T. Ishigaki, H. Tanaka, M. Kurihara, N. Ohashi, J.G. Li, S. Maruyama, and Y. Moriyoshi: "Influence of Sulpher and Fluorine Containing Thermal Plasma Treatment of Graphite Powders on the Anode Performance of Lithium-Ion Rechargeable Battery", ISPC-17 ID91 (2005)

(2) Y. Tanaka and T. Sakuta: "Investigation on plasma-quenching efficiency of various gases using the inductively coupled thermal plasma technique: effect of various gas injection on Ar thermal ICP", *J. Phys. D: Appl. Phys.*, Vol.35, pp.2149–2158 (2002)

(3) H. Nishiyama, Y. Muro, and S. Kamiyama: "Control of gas temperature and velocity fields of an RF induction thermal plasma by injecting secondary gas", *J. Phys. D. Appl. Phys.*, Vol.29, pp.2634–2643 (1996)

(4) M. Cai, D.A. Hayder, A. Montasir, and J. Mostaghimi: "Computer simulation of argon-nitrogen and argon-oxygen inductively coupled plasmas.", *Spectrochim. Acta.*, Vol.52B, pp.369–386 (1997)

(5) F. Bourg, S. Pellerin, D. Morvan, J. Amouroux, and J. Chapelle: "Spectroscopic diagnostic of an argon-hydrogen RF inductive thermal plasma torch at atmospheric pressure used for silicon hydrogenation", *J. Phys. D: Appl. Phys.*, Vol.35, pp.2281–2290 (2002)

(6) Y. Tanaka: "Two-temperature chemically non-equilibrium modeling of high-power Ar-N_2 inductively coupled plasmas at atmospheric pressure", *J. Phys. D: Appl. Phys.*, Vol.37, pp.1190–1205 (2004)

(7) M.W. Chase, *et al.*: JANAF thermodynamical tables, 3rd Ed., Vol.14, NSRDS (1985)

(8) Y. Tanaka, K.C. Paul, and T. Sakuta: "Thermodynamic and .Transport Properties of O_2/N_2 Mixture at Different Admixture Ratio", *T. IEE Japan*, Vol.120-B, pp.24–30 (2000)

Sharif Abdullah Al-Mamun (Student Member) was born on September 1, 1975. He obtained B.Sc. Engineering from Bangladesh Institute of Technology, Chittagong, Bangladesh (presently Chittagong University of Engineering & Technology) in 2001. On the same year he joined as a lecturer at the same department of Electrical & Electronic Engineering. Now, he is pursuing M.S. at Kanazawa University. His research interest includes mixed gas ICTP and its applications.

Yasunori Tanaka (Member) was born on 1970 in Japan. He received B.S., M.S., and Ph.D. degrees in electrical engineering from Nagoya University, Japan, in 1993, 1995 and 1998, respectively. In April 1998, he was appointed a Research Associate at Kanazawa University, Japan. He has been working as an Associate Professor since August 2002 at that university. His research interests include arc interruption phenomena and thermal plasma applications.

Yoshihiko Uesugi (Member) He was born in 1955 in Japan. He received a B.E., M.E. and D.E. degrees from Nagoya University in 1977, 1979 and 1983, respectively. After working as a research staff of Japan Atomic Energy Research Institute and an associate professor of Nagoya University, he is presently a professor of Graduate School of Natural Science in Kanazawa University. His research interests are high power plasma generation and application, and megnetic fusion experiments.